RSC Advances

ROYAL SOCIETY OF CHEMISTRY

www.rsc.org/advances

TOC

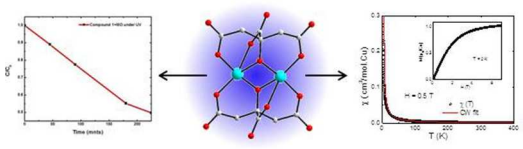

A new paramagnetic and semiconductor copper citrate dimer exhibits photocatalytic behaviour towards the organic dye degradation.

Journal Name

RSCPublishing

ARTICLE

Synthesis, Structure, Photocatalytic and Magnetic Properties of an Oxo-bridged Copper Dimer

Cite this: DOI: 10.1039/xoxxoooooox

Raja Ghosh,[a] Asha K S,[a] Saied Md Pratib,[b] Ayan Datta,[b] Ramesh Nath,[c] Sukhendu Mandal*[a]

Received ooth January 2012,
Accepted ooth January 2012

DOI: 10.1039/xoxxoooooox

www.rsc.org/

Dimeric copper complex, $[GuH]_4[Cu^{II}_2(Cit)_2].2H_2O$ (where GuH = monoprotonated guanidine and Cit = citrate anion) was synthesized solvothermally and characterized by single crystal-X-ray diffraction. The Cu atoms are bridged by alkoxide oxygen atoms of the citrate ligand forming the dimer. The Cu atom adopts distorted square pyramidal geometry. Two CuO_5 units are connected edge-wise to form the dimer which is capped by the citrate ligand. This molecular dimer is strongly H-bonded with guanidine cation and water molecule to form supramolecular structure. The optical band gap energy data exhibits its semiconductor behavior. We have explored this material as a photocatalyst for the degradation of organic dye. The magnetic measurements show that compound **1** behaves like a paramagnet. Detailed theoretical investigations reveal that inter-molecular H-bonding is responsible for the stability of this structure.

The increasing interest in dimer, trimer, tetramer and higher-membered metal complexes is due to their unusual properties and their potential as single-molecule magnets (SMMs).[1,2] The focus on cluster-based coordination polymers have increased rapidly in recent years due to their richness in chemistry.[3] Much efforts have been devoted to the construction of such compounds with tunable properties through the design of metal clusters as secondary building units (SBUs) and organic ligands as linkers.[4] Metal carboxylate clusters due to their thermal stability and multiple bonding centers have proven their value to construct hierarchy of structures.[5] Recently Lin et al. showed that increase in size of the Zn-based SBU clusters lead to a red shift in band gap energy of metal organic framework (MOFs).[4a] They also proved that conjugation of carboxylate linkers have pronounced effect on MOFs' band gap energy.[4a] Hendon et al. reported that functionalization of ligand can lead to a change in band gap energy.[4b] In this context we have shown that substitution of metal ion in MOFs can significantly modify the band gap energy.[6] Linked clusters are stabilized through strong covalent interactions while for an isolated cluster, H-bonding plays a crucial role in its stability, which can affect the properties of the cluster when these are crystallized with protonated amine and water molecules.[7] Due to its unique binding mode citric acid can stabilize metal cluster with variation in metal coordination number.[8] The citrate ligand is able to generate metal-oxocubane structures that are of particular interest for the creation of SMMs.[8] The literature on dimeric cluster based on citrate ligand is rare.[9] Cluster chemistry is fascinating due to their magnetic behavior and in most of the cases it behave like a SMM. The optical behavior of clusters have not been explored much.[10] We are interested in exploring the semiconductor properties of clusters based materials.[11] A new application of semiconductor cluster is photocatalysis and some results have demonstrated that these are efficient photocatalysts for the degradation of organic dyes.[12] There is always a great demand to correlate the structure-properties relationship for these type of materials.[13] To do this we have synthesized a dimeric copper cluster linked by citrate ligand. The cluster is stabilized by H-bonding with protonated guanidine cation and water molecule. Here we present the synthesis, single crystal structure, DFT calculations, optical band gap energy, photocatalysis, magnetism of $[GuH]_4[Cu^{II}_2(cit)_2].2H_2O$, **1**.

Experimental Section

General: All chemicals were of reagent-grade quality and purchased from Sigma-Aldrich and used as received without further purification. The elemental analysis (C, H, and N) was carried out on vario MICRO elementar instrument. The FT-IR spectrum was recorded from KBr pellets in the range of 400-4000 cm^{-1} on SHIMADZU FT-IR spectrometer. The TGA was performed on Perkin-Elmer TG-7 analyzer in flowing argon with a heating rate of 5^0 C per minute. Powder X-ray diffraction data was collected on PAN analytical machine with CuKα radiation (λ = 1.54060 Å) and single crystal X-ray diffraction data was collected on Bruker APEX-II machine with MoKα = 0.71073 Å).

Synthesis

In a conventional synthesis, citric acid (1.00 g, 5.2 mmol) and $Cu(NO_3)_2$. $2.5H_2O$ (1.26 g, 5.2 mmol) was dissolved in distilled water (50 ml). To this, guanidine carbonate (3.78 g, 20.8 mmol) was added. Mixture was sonicated for two minutes. A portion of the resulting blue solution was kept uncovered in petri dish and after 24 hours blue colored crystals were formed. The residue was washed with methanol several times to remove the impurity. Yield was 85% based on metal.

Single Crystal Structure Determination

A suitable crystal of **1** was carefully selected under a polarizing microscope and glued to a thin glass fiber. The single crystal diffraction data was collected on a Bruker AXS APEX-II CCD diffractometer at 298(2) K. The X-ray generator was operated at 50 kV and 35 mA using MoKα (λ = 0.71073Å) radiation. Data was collected with ω scan width of 0.3°. A total of 606 frames were collected in three different settings of φ (0°, 90°, 180°) keeping the sample to-detector distance fixed at 6.03 cm and the detector position (2θ) fixed at -25°. Pertinent structural parameters of **1** are presented in Table S1.

The data was reduced using SAINTPLUS,[14] and an empirical absorption correction was applied using the SADABS program.[15] The crystal structure was solved by direct methods using SHELXS97 and refined using SHELXL97 present in the WinGx suite of programs (Version 1.63.04a).[16] We have located the hydrogen atoms to lattice-water and guanidine molecules in **1**. For the final refinement, the hydrogen atoms were placed in geometrically ideal positions and refined using the riding mode. The last cycle of the refinement included atomic positions, anisotropic thermal parameters for all the non-hydrogen atoms, and isotropic thermal parameters for all the hydrogen atoms. Full-matrix-least-squares structure refinement against F^2 was carried out using the WINGX [17] package of programs.

CCDC-978079 contains the crystallographic data for **1**. This data can be obtained free of charge from The Cambridge Crystallographic Data Centre (CCDC) via www.ccdc. cam.ac.uk/data_request/cif

Characterizations

Initial characterizations were carried out by elemental analysis, powder X-ray diffraction (XRD), thermogravimetric analysis (TGA), and IR spectroscopic studies. Elemental analysis of the crystals was carried out using a CHNS analyzer. Elemental analysis calculated (%) for **1**: C 24.90, H 3.66, N 21.78; found: C 24.82, H 3.75, N 21.87.

The powder XRD pattern was recorded on crushed single crystals in the 2θ range 5-50°. The XRD pattern indicated that the product is a new material; the pattern was entirely consistent with the simulated XRD patterns generated based on the structures determined using single-crystal XRD (Figure S1). The TGA for as synthesized materials showed a weight-loss step at (25–100 □ C) which is due to the loss of lattice water molecules (Figure S2). The second weight loss after 250 □ C is due to loss of amine molecules and citrate ligands. IR spectroscopic studies were carried out in the range 400-4000 cm^{-1} using the KBr pellet method (Perkin-Elmer, SPECTRUM 1000). IR spectrum exhibited typical peaks corresponding to the amine molecule, the carboxylate moiety, and the lattice-water molecule in their respective bands (Table S2 and Figure S3).

Optical Band Gap Energy Measurements

The diffuse reflective spectra of compound **1** and metal precursor $Cu(NO_3)_2.2.5H_2O$ were collected on a Shimadzu UV/Vis/NIR spectrophotometer using $BaSO_4$ as reference material. The room temperature diffuse reflectance spectra was measured and converted to a Kubelka–Munk function from which the band gap energy of the compound **1** and metal precursor, $Cu(NO_3)_2.2.5H_2O$ were estimated.[18] This two-flux model which considers only diffuse light is used to determine the absorption coefficient from a surface that both scatters and absorbs incident radiation. For a crystalline solid with a band gap (E_{bg}), the frequency (ν) dependence of the absorption coefficient (κ) can be approximated as

$$\kappa(\nu) = \frac{B_T(h\nu - E_{bg})^n}{h\nu},$$

Where B_T is a constant derived from the square of the averaged dipolar momentum matrix element and n is equal to 0.5 and 2 for *direct* and *indirect* band gap transitions, respectively.[19] Using the above equation, the band gap of a material can be obtained by extrapolating to x-axis with the linear fit to a plot of $(khv)^{1/n}$ vs hν.

Computational Section

To understand the nature of interaction among copper citrate framework, protonated guanidine molecules and water molecules in **1**, the ground state of all the individual molecules and the compound **1** were optimized in gas phase using the hybrid DFT functional M06-2X [20,21] as implemented in Gaussian 09 with 6-31+G(d,p)[22] (for all atoms) and 6-31+G(d,p) (H, C, N, O), LANL2DZ (Cu) basis set schemes.[23] The hybrid meta exchange-correlation functional, M06-2X from Truhlar's group has been successful in accounting for medium – range electron correlation in charge – transfer systems and correctly incorporates dispersion forces.[24,25] Additional harmonic frequency calculations were performed for ensuring that the structures do not correspond to saddle – points. All the computed structures have real vibrational modes in the ground state structures. Basis Set Superposition Error (BSSE) was corrected using the Counterpoise (CP) correction scheme.[26]

Photocatalytic Activity Study

The photocatalytic activities of compound **1** was evaluated by the degradation of methyl orange (MO) in aqueous solution. A 50 mL of MO aqueous solution with a concentration of 300 ppm was mixed with 100 mg of compound **1**. A lamp (365 nm) was used as the UV source. During the degradation, the mixture was stirred continuously by a magnetic stirrer. At regular time intervals, 1 mL of the solution was sampled, filtered and diluted to 10 mL in a volumetric flask. The UV-Vis absorption spectra of MO in aqueous solution were measured by UV-Vis spectroscopic method.

Magnetic Measurement

Magnetic susceptibility (χ) as a function of temperature (T) was measured at an applied field (H) of 0.5 T. A magnetization (M) isotherm (M vs. H) was also measured at T=2 K. Both the measurements were done using a SQUID-VSM [Quantum Design].

Results and Discussion

Structural Description

The compound $[GuH]_4[Cu^{II}_2(cit)_2].2H_2O$, **1** crystallizes in an orthorhombic system with space group *Pbca*.[9a] The asymmetric unit

contains one copper atom, one molecule of citrate ligand, two guanidine cations and one lattice water molecule. Each copper atom of the dimeric unit is five coordinated and the geometry around the copper ion is distorted square-pyramidal (Figures 1, S4 and Table S3). Each Cu has a distorted square pyramidal type of geometry as ascertained by Reedijk's τ factor of 0.266 (τ =0 for a square pyramid, and τ = 1 for a trigonal bipyramid).[27] The structural index τ is defined as (α – β)/60, where α and β being the two largest angles. The structure of **1** consists of two CuO_5 units which are connected edge-wise and capped by two citrate ligands forming the $[Cu_2(cit)_2]^{4-}$ dimer. The bridging Cu_2O_2 unit is planar with a crystallographic inversion center. The dimer having six pendent C = O bonds from two citrate ligands which is a potential moiety for forming hydrogen bonding. The guanidinium counter cation and water molecules are involved in an extensive H-bonding network with the citrate ligand oxygen atoms of C = O bonds and forming the H-bonded supramolecular structure (Figures 2 and S5).

Compound **1** is highly stable due to the presence of a network of ten hydrogen bonds (Figure 3). The encapsulated water molecule within the framework of 1 contains both donor (N-H...O = 2.17 Å and N-H...O = 2.06 Å) and acceptor (O-H...O = 1.99 Å) type H-bonding. Using M06-2X DFT functional with 6-31+g(d,p)basis and with mixed basis, the stabilization energies are -290.2 kcal/mol and -279.2 kcal/mol, respectively. BSSE corrected stabilization energies for the complex with pure and mixed basis set are -282.7 kcal/mol and -272.6 kcal/mol, respectively.

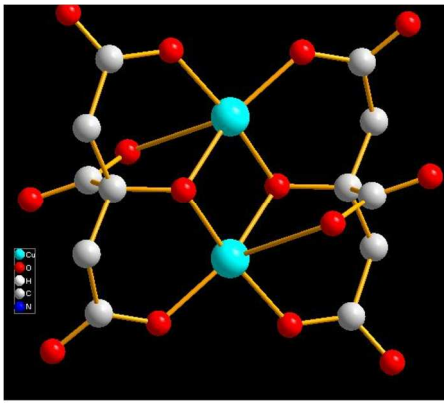

Figure 1. The structure of **1**, $[GuH]_4[Cu^{II}_2(Cit)_2]$. $2H_2O$, showing two Cu ions bridged by oxygen atoms.

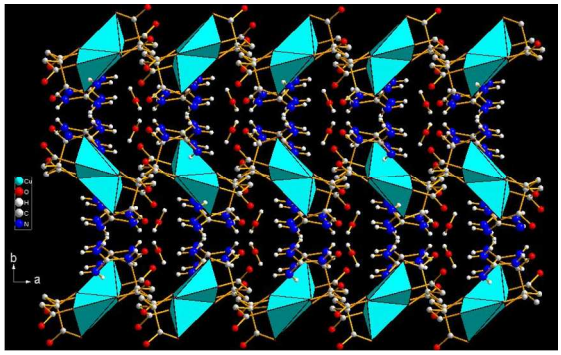

Figure 2. The supramolecular structure of **1**, which is formed by the H-bond interactions between copper citrate, protonated amine and lattice water molecules. (For clarity H-bonds were not shown).

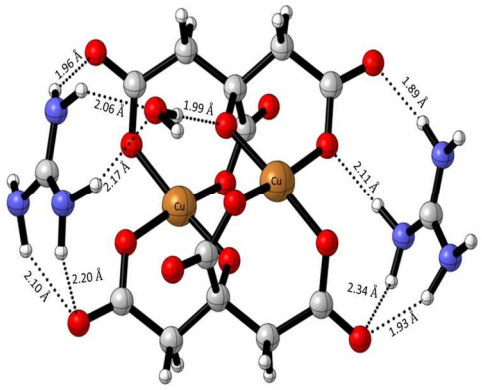

Figure 3. Ground state optimized structures (at M06-2X/6-31+G(d,p level of theory) in gas phase.

Band Gap Energy Measurement

We have collected the diffuse reflectance UV-Vis spectra of the powder sample of **1** in order to measure the band gap energy (E_{bg}), which was confirmed as the intersection point between the energy axis and the line extrapolated from the linear portion of the adsorption edge in a plot of the Kubelka–Munk function vs. energy. As shown in figure S6, the optical absorption associated with E_{bg} can be assessed at 2.30 eV for **1**. Khanna and coworkers, from the theoretical calculations, have shown that this kind of materials exhibit flat bands which indicates indirect band gap in the material.[10] The reflectance spectra indicate that compound **1** is a semiconductor material and can be used as a photocatalyst. We have measured the band gap energy of metal precursor, $[Cu(NO_3)_2.\ 2.5H_2O]$ to find the role of anion towards the band gap energy. The result shows that band gap energy increases from metal precursor (E_{bg} = 2.24 eV) to compound **1** (E_{bg} = 2.30 eV) (Figure S6). It is evident that for such metal complexes the conduction band is influenced by the metal ion while the valence band contribution comes from the anionic ligand.[4b, 28] In this case though the metal ion is same, there is a difference in their coordination (tetrahedral for $Cu(NO_3)_2$ and distorted square-pyramidal for compound **1**) (Figure S7) which apparently leads to a change in position of their conduction bands. Secondly due to different electron withdrawing ability of the ligands (NO_3 vs citrate) the valence band positions also varies. These combined effects may be responsible for the difference in band gap energy between precursor and compound **1**.

The band gap energy of **1** (E_{bg} = 2.30 eV) underscores its potential as a photocatalyst. To study the photocatalytic activity of compound **1** in detail, we have taken methyl orange (MO) as a model dye pollutant in aqueous media to demonstrate the efficacies of the photocatalytic behavior. The photocatalytic performance of compound **1** was estimated from the variation of the color in the reaction system by monitoring the absorbance (at λ = 460 nm) characteristic of the target MO which directly relate to the structural changes of their chromophore. Control experiments suggest that compound **1** can degrade the dye in presence of UV light only (Figure 4).

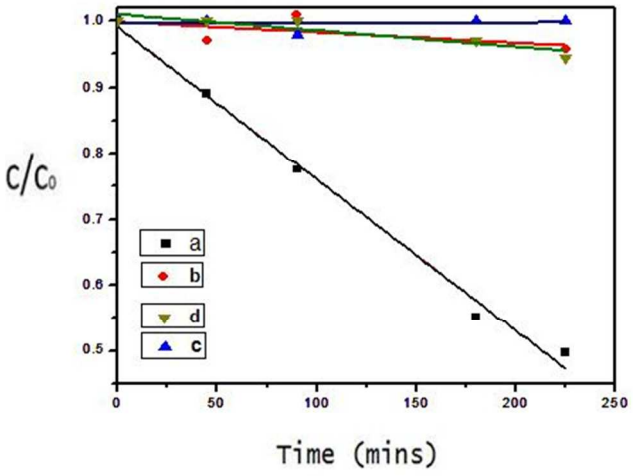

Figure 4. Degradation profiles of Methyl Orange (MO) dye with an initial concentration of 300 ppm (a) catalyst under UV, (b) under UV (without catalyst), (c) Visible light (without catalyst), (d) only catalyst (under visible light).

To quantify the reactions, the kinetics was determined by the Langmuir-Hinshelwood (L-H) kinetic. This can be written as $r_0 = k_0C_0/(1 + K_0C_0)$, where r_0 is the initial rate, C_0 is the initial concentration of the dye, k_0 is the kinetic rate constant, and parameter K_0 represents the equivalent adsorption coefficient. The plot of the reciprocal initial degradation rate ($1/r_o$) with the reciprocal of the initial dye concentration ($1/C_0$) by using **1** is shown in Figure 5. The values of the parameters, k_0 and K_0, for the photocatalytic degradation of MO, obtained from the slope and the intercept of the linear plot, are 0.006 min^{-1} and 0.0014 ppm^{-1}, respectively. As the parameter, K_0, represents the adsorption equilibrium coefficient, the low value of K_0 can be attributed to negligible adsorption. This is also confirmed by powder XRD of the catalyst after the photocatalytic degradation experiments, which clearly indicated that the structure remained the same and no adsorption was observed (Figure S8).

To understand the photocatalytic degradation of the organic dye, we employ a simple approach based upon valence band (VB) and conduction band (CB) consideration. The initial process of photocatalysis is the generation of electron– hole pairs in the compound **1**. After absorption of energy equal to or greater than the band gap of compound **1** (E_{bg} = 2.30 eV), the electrons (e^-) are excited from VB to the CB, leaving the holes (h^+) in the VB. The electrons and holes migrate to the surface of the compound **1**, then the photoinduced energy transfers to the adsorbed species. The adsorbed oxygen (O_2) is reduced to oxygen radicals ($^{\bullet}O_2^-$), and finally transforms into hydroxyl radicals ($^{\bullet}OH$). Hydroxyl (OH^-) ions adsorbed on the surface of **1** interact with the hole (h^+) generating hydroxyl radicals ($^{\bullet}OH$) Hydroxyl radicals ($^{\bullet}OH$) have the ability to decompose methyl orange effectively (scheme 1).[29]

The molar magnetic susceptibility (χ_m) of the powder sample of **1** was measured in the temperature range 2-400 K (Figure 6). The χ_m value increases slowly as the temperature decreases in a Curie-Weiss (CW) manner reflecting the paramagnetic nature of the compound. No indication of any magnetic ordering was found down to 2 K.

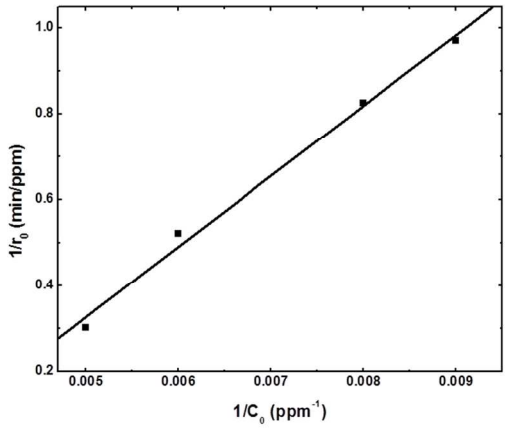

Figure 5. Variation of the photodegradation rate with concentration of MO.

In order to extract the magnetic parameters we fitted the data using the following expression

$\chi_m = \chi_0 + C/(T - \Theta)$, where χ_0 is the temperature-independent contribution and the second term is the Curie-Weiss (CW) law with the Curie constant, $C [= Ng^2\mu_B^2S(S+1)/3k_B]$ and Weiss temperature Θ. The effective moment is given by $\mu_{eff} = g[S(S + 1)]^{1/2}\mu_B$. The data in the whole temperature range was fitted with the parameters $\chi_0 = -4.709 \times 10^{-4}$ cm^3/mol.Cu, C = 0.559 cm^3 K/mol.Cu, and θ = 3.3 K. This value of C corresponds to μ_{eff} = 2.1 μ_B, which is slightly higher than the expected spin-only value (1.73 μ_B) for S = 1/2 of Cu^{2+} assuming g = 2. The negligible value of Θ suggests that the interaction between the Cu spins is very weak.

The M vs. H curve at T = 2 K (inset of Figure 6) increases almost linearly at low fields and then saturates at 7 T to a saturation magnetization M_s = 1 μ_B. For S=1/2 system the saturation magnetization is expected to be 1 μ_B ($M_s = gS\mu_B$). The overall shape of the curve is similar to that expected for a paramagnet.[30]

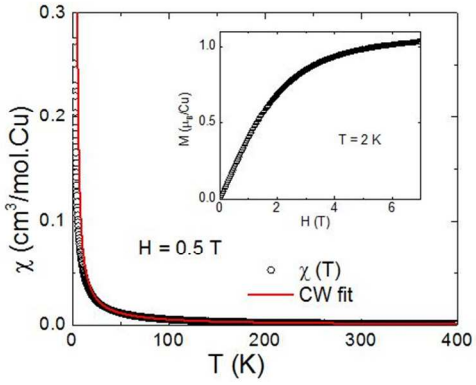

Figure 6. Temperature variation of the molar magnetic susceptibility (χ_m) for **1**. The inset shows the corresponding magnetization (M) *vs* field (T) plot.

Nearly negligible super-exchange between copper centers of dimer complexes which exhibit a square pyramidal geometry can be explained in terms of Hoffmann's theory.[31] From the structural analysis it was found that copper ions are having distorted square

pyramidal geometry ($\tau = 0.266$). In such geometry the $d_{x^2-y^2}$ orbitals of copper ions and 2p orbitals of oxygen atom which are responsible for super-exchange are aligned orthogonal to each other. Due to this kind of orbital arrangements the super-exchange between copper ions is negligible which is evident from the experiment.

Conclusions

In conclusion, we have synthesized dimeric copper compound, which is characterized by single crystal X-ray diffraction, elemental analysis, IR and TGA analysis. Theoretical calculations underscore the role of H-bonding towards the stability of **1**. The optical band gap energy measurement shows that the compound behaves like a semiconductor. The semiconductor behavior of **1** was explored as a photocatalyst. It shows good photocatalytic activity towards MO degradation. Magnetic measurement exhibits its paramagnetic behavior. The square-pyramidal geometry of the copper ion in **1** is responsible for the lack of super-exchange.

Acknowledgments

This work was funded by IISER-TVM and Science and Engineering Research Board (SERB), Govt. of India through a grant SB/S1/IC-14/2013.
The authors are grateful to Prof. E. D. Jemmis, former director and Prof. V. Ramakrishnan, present director for their encouragement. We also would like to thank Prof. A. V. Mahajan and Susanta Kundu (IIT Bombay) for magnetic measurements. R.G acknowledges DST for Inspire fellowship and A. K S acknowledges CSIR for JRF, respectively.

Notes and references

[a] School of Chemistry
Indian Institute of Science Education and Research Thiruvananthapuram, Kerala, India-695016
Fax: (+91) 471-2597-438
E-mail: sukhendu@iisertvm.ac.in
Homepage: http://iisertvm.ac.in/~sukhendum
[b] Department of Spectroscopy,
Indian Association for the Cultivation of Science,
Kolkata, West Bengal, INDIA-700032
[c] School of Physics
Indian Institute of Science Education and Research Thiruvananthapuram, Kerala, India-695016

Electronic Supplementary Information (ESI) available: Tables for IR, selected bond lengths and angle, figures for Cu geometry, H-bonded network, band gap energy, figure for metal precursor, and catalysis plots powder X-ray diffraction pattern, TGA, IR plots and scheme for photocatalytic mechanism. For ESI and cif see DOI: 10.1039/b000000x/

1. C. J. Milios, A. Vinslava, W. Wernsdorfer, S. Moggach, S. Parsons, S. P. Perlepes, G. Christou, E. K. Brechin, *J. Am. Chem. Soc.*2007, **129**, 2754.
2. I Mirebeau, M. Hennion, H. Casalta, H. Andres, H. U. Güdel, A. V. Irodova, A. Caneschi, *Phys. Rev. Lett.* 1999, **83**, 628.
3. K. N. Ferreira, T. M. Iverson, K. Maghlaoui, J. Barber, S. Iwata, *Science* 2004, **303**, 1831.
4. (a) C-K. Lin, D. Zhao, W-Y. Gao, Z. Yang, J. Ye, T. Xu, Q. Ge, S. Ma, D J. Liu, *Inorg. Chem.* 2012, **51**, 9039; (b) C. H. Hendon, D. Tiana, M. Fontecave, C. Sanchez, L. D'arras, C. Sassoye, L. Rozes, C. Mellot-Draznieks, A. Walsh, *J. Am. Chem. Soc.* 2013, **135**, 10942.
5. M. Eddaoudi, D. B. Moler, H. L. Li, B. L. Chen, T. M. Reineke, M. O'Keeffe, O. M. Yaghi, *Acc. Chem. Res.* 2001, **34**, 319.
6. A. K. S, A. M. Gupta, R. Ghosh, A. George, S. Mandal, Submitted elsewhere.
7. S. Neeraj, S. Natarajan, *Cryst. Growth & Desgn.*2001, **1**, 491.
8. (a) T. A. Hudson, K. J. Berry, B. K. Moubaraki, S. Murray, R. Robson, *Inorg. Chem.* 2006, **45**, 3549; (b) B. Moubaraki, K. S. Murray, T. A. Hudson, R. Robson, *Eur. J. Inorg. Chem.* 2008, 4525; (c) K. W. Galloway, A. M. Whyte, W. Wernsdorfer, J. Sanchez-Benitez, K. V. Kamenev, A. Parkin, R. D. Peacock, M. Murrie, *Inorg. Chem.* 2008, **47**, 7438.
9. (a) D. M. Boghaei, M. M. Najafpour, *Anal. Sci.: X-Ray Struct. Anal. Online,*2007, **23**, x123; (b) K. W. Galloway, S. A. Moggach, P. Parois, A. R. Lennie, J. E. Warren, E. K. Brechin, R. D. Peacock, R. Valiente, J. González, F. Rodríguez, S. Parsons, M. Murrie, *Cryst. Eng. Comm*, 2010, **12**, 2516.
10. (a) S. Mandal, A. C. Reber, M. Qian, P. S. Weiss, S. N. Khanna, A. Sen, *Acc. Chem. Res.*, 2013, **46**, 2385; (b) M. Qian, A. C. Reber, A. Ugrinov, N. K. Chaki, S. Mandal, H. M. Saavedra, S. N. Khanna, A. Sen, P. S. Weiss, *ACS Nano* 2010, **4**, 235; (b) N. K. Chaki, S. Mandal, A. C. Reber, M. Qian, H. M. Saavedra, P. S. Weiss, S. N. Khanna, A. Sen, *ACS Nano* 2010, **4**, 5813; (c) S. Mandal, A. C. Reber, M. Qian, R. Liu, H. M. Saavedra, S. Sen, P. S. Weiss, S. N. Khanna, A. Sen, *Dalton Trans.* 2012, **41**, 12365.
11. C. G. Silva, A. Corma, H. García, *J. Mater. Chem.*, 2010, **20**, 3141.
12. (a) P. Mahata, G. Madras, S. Natarajan, *J. Phys. Chem. B* 2006, **110**, 13759; (b) P. Mahata, T. Aarthi, G. Madras, S. Natarajan, *J. Phys. Chem. C* 2007, **111**, 1665.
13. (a) A. K. Paul, U. Sanyal, S. Natarajan. *Cryst. Growth. & Desgn.*2010, **10**, 4161; (b) P. Ramaswamy, A. Datta, S. Natarajan, *Eur. J. Inorg. Chem.* 2008, 1376.
14. SMART (V 5.628), SAINT (V 6.45a), XPREP, SHELXTL; Bruker AXS Inc.: Madison, WI, 2004.
15. G. M. Sheldrick, Siemens Area Correction Absorption Correction Program; University of Göttingen: Göttingen, Germany, 1994.
16. G. M. Sheldrick, SHELXL-97 Program for Crystal Structure Solution and Refinement; University of Göttingen: Göttingen, Germany, 1997.
17. J. L. Farrugia, *J. App. Crystallography*. 1999, **32**, 837.
18. P. Kubelka, *J. Opt. Soc. Am.*1948, **38**, 448.
19. N. Laidani, R. Bartali, G. Gottardi, M. Anderle, *J. Phys.: Condens. Matter* 2008, **20**, 015216.
20. Y. Zhao, N. E. Schultz, D. G. Truhlar, *J. Chem. Theory and Comput.* 2006, **2**, 364.
21. Y. Zhao, D. G. Truhlar, *Acc. Chem. Res.*2008, **41**, 157.
22. P. C. Hariharan, J. A. Pople, *Theor. Chim.Acta* 1973, **28**, 213.
23. M. J. Frisch, et al. Gaussian 09 Rev 09.A0; Gaussian, Inc.: Wallingford, CT, 2009.
24. (a) A. K. Jissy, A. Datta, *J. Phys Chem. B* 2010, **114**, 15311. (b) S. A. Abraham, D. Jose, A. Datta, *Chem. Phys. Chem,* 2012, **13**, 695.
25. (a) A. Nijamudheen, D. Jose, A. Shine, A. Datta, *J. Phys. Chem. Lett.* 2012, **3**, 1493. (b) A. K. Jissy, U. P. M. Ashik, A. Datta, *J. Phys. Chem. C*, 2011, **115**, 12530. (c) D. Jose, A. Datta, *Cryst. Growth. & Desgn.* 2011, **11**, 3137.
26. S. F. Boys, F. Bernardi, *Mol. Phys.*1970, **19**, 553.

27. A. W. Addison, T. N. Rao, J. Reedijk, J. V. Rijn, G. C. Verschoor, *J. Chem. Soc*., *Dalton Trans*. 1984, 1349.
28. (a) C. H. Hendon, D. Tiana, A. Walsh, *Phys. Chem. Chem. Phys*.2012, **14**, 13120. (b) J. H. Choi, H. J. Jeon, K. M. Choi, J. K. kang, *J. Mater. Chem.* 2012, **22**, 10144.
29. (a) C. Galindo, P. Jacques, A. Kalt, *J. Photochem. Photobiol., A*, 2000, ***130***, 35; (b) J. Joseph, H. Destaillats, H. Hung, M. Hoffmann, *J. Phys. Chem. A*, 2000, **104**, 301.
30. C. Kittel, *Introduction to Solid State Physics*, 4th ed. (Wiley, New York, 1966).
31. P. J. Hay, J. C. Thibeault, R. Hoffmann, *J. Am. Chem. Soc.* 1975, **97**, 4884.

